

PARAMETRIC DYNAMIC ANALYSIS OF TENSEGRITY CABLE-STRUT DOMES¹

PAULINA OBARA, MARYNA SOLOVEI, JUSTYNA TOMASIK

Kielce University of Technology, Faculty of Civil Engineering and Architecture, Kielce, Poland

correspondence author Maryna Solovei, e-mail: msolovei@tu.kielce.pl

The paper contains a parametric dynamic analysis of cable-strut domes. The special structures named tensegrity are considered. Two qualitative different tensegrity domes, i.e., the Geiger dome and the Levy dome are taken into account. The aim of the study is to compare the dynamic behaviour of such structures. The first stage of analysis involves the identification of initial prestress forces (system of internal forces, which holds structural components in stable equilibrium) and infinitesimal mechanisms. The second stage focuses on calculating natural frequencies, while in the last, the impact of time-independent external loads on vibrations is studied. The influence of initial prestress and external load on the dynamic response of the structures is considered. A geometrically non-linear model is used to analysis. Presented considerations are crucial for the next step in the analysis, i.e., dynamic stability analysis of the behaviour of tensegrity structures under periodic loads.

Keywords: tensegrity dome, initial prestress, infinitesimal mechanisms, natural vibrations, free vibrations

1. Introduction

The tensegrity steel domes are special cable-strut trusses. These structures are characterized by a system of internal forces, which holds structural components in stable equilibrium (a self-balanced system of internal forces, self-stress state, initial prestress). Additionally, some of these structures are also characterized by the presence of infinitesimal mechanisms, which are stabilized by a self-balanced system of internal forces. In such cases, a modification of the initial prestress allows for controlling static and dynamic parameters of the structure. Low material demand, lightness of the system, and resistance to various types of loads are the main advantages of these structures. The most common are two tensegrity domes, i.e., the Geiger dome (Geiger, 1988) and the Levy dome (Levy, 1989). In the years 1990-2022, according to Google Scholar, the appearance of the Geiger dome in different articles counts more than 10 000 and more than 18 000 of Levy's dome. Both structures consist of load-bearing systems represented by flat or spatial girders connected with additional longitudinal cables. The approach of tensegrity dome is used for long-span roofs (Levy, 1994; Oribasi *et al.*, 2002) and covers (Geiger *et al.*, 1986; Levy *et al.*, 2013).

Practical application of tensegrity domes requires a thorough examination of static and dynamic properties, as well as overall behaviour of the structure. Most of the research to date focuses on layout design (Rebielak, 2000; Yuan *et al.*, 2007), form-finding methods (Lee *et al.*, 2009), or shape optimization (Kawaguchi *et al.*, 1999; Zhang and Feng, 2017). A smaller number of studies focused on static parameters of tensegrity structures (Shen *et al.*, 2021; Sun *et al.*, 2021; Obara *et al.*, 2023a), and only a few on the dynamic behaviour of dome systems (Obara, 2019; Kim and Sin, 2014; Atig *et al.*, 2017). Due to a non-conventional shape, the complete dynamic

¹Paper presented during PCM-CMM 2023, Gliwice, Poland

analysis of tensegrity domes can be challenging. Some papers contain an initial dynamic analysis of the Geiger dome (Kim and Sin, 2014; Qin *et al.*, 2023).

The analysis of the literature shows that the vast majority of works concerns tensegrity design, the search for stable forms, optimization algorithms, methods of controlling the shape of tensegrity structures under the influence of external loads, and discusses the use of these structures. Against this background, parametric analysis evaluating the influence of the initial prestress on dynamic properties of tensegrity structures is the subject of few studies. In addition, these works relate to specific solutions. The first attempt to fill this gap was the paper (Obara and Solovei, 2023). The influence of initial prestress on the natural frequency for Geiger domes was determined. Two cases of configurations (with a closed and open upper section) were considered. Additionally, two variants of the nature of a dome (regular and modified) were taken into account to compare the dynamic behaviour of domes. In turn, this paper contains a comparison of the dynamic behaviour of the two most popular, qualitatively different, types of tensegrity domes i.e., the Levy and Geiger domes. First, the system of internal forces, which holds structural components in stable equilibrium (initial prestress), and infinitesimal mechanisms are identified. Next, the influence of initial prestress on frequencies is determined. The consideration includes natural and additionally free vibrations. The impact of time-independent external loads on the vibrations is analyzed. The load is treated as an initial disturbance of the equilibrium state, i.e., as imposition of the initial conditions, hence the frequencies are called free. To evaluate this behaviour, a geometrically non-linear model is used. The presented parametric considerations, among others, lead to an answer to the question of how the initial prestress and external load influence the dynamic response of the structure. Additionally, they are crucial for the dynamic stability analysis of the behaviour of tensegrity structures under periodic loads, which will be the subject of the next considerations.

2. Material and methods

Tensegrity domes are described n -element ($e = 1, 2, \dots, n$) spatial cable-strut trusses with m degrees of freedom $\mathbf{q} \in \mathbb{R}^{m \times 1}$. The elasticity of elements e are described by the elasticity matrix $\mathbf{E} \in \mathbb{R}^{n \times n}$

$$\mathbf{E} = \text{diag} \left[\frac{E_1 A_1}{L_1} \quad \frac{E_2 A_2}{L_2} \quad \dots \quad \frac{E_n A_n}{L_n} \right] \quad (2.1)$$

where E_e is Young's modulus, A_e is across-sectional area and L_e is length of the element. In turn, geometry is described by the compatibility matrix $\mathbf{B} \in \mathbb{R}^{n \times m}$, which can be determined using formalism of the finite element method (Zienkiewicz and Taylor, 2000). Additionally, in contrast to traditional steel domes, tensegrity domes are characterized by a self-balanced system of internal forces (self-stress state). The first step of the analysis of tensegrity structures relies on the identification of the self-stress state. The most frequently used methods are the force density method (Zhang and Ohsaki, 2006), dynamic relaxation (Bel Hadj *et al.*, 2010), energy optimization (Li *et al.*, 2011), reduced coordinates method (Arsenault and Gosselin, 2005), iteration method (Ma *et al.*, 2018), genetic algorithm (Obara *et al.*, 2023b), singular value decomposition of the force density and equilibrium matrices (Tran and Lee, 2013) or of the compatibility matrix (Gilewski *et al.*, 2016). Since the self-stress state does not depend on geometrical and mechanical characteristics and on an external load, one of the simplest methods to identify it is spectral analysis of the matrix $\mathbf{B}\mathbf{B}^T \in \mathbb{R}^{n \times n}$. The self-stress state is considered as an eigenvector $\mathbf{y}_S \in \mathbb{R}^{n \times 1}$ related to the zero eigenvalue of the matrix $\mathbf{B}\mathbf{B}^T$ (Obara, 2019; Obara and Solovei, 2023). The self-equilibrium system of longitudinal forces $\mathbf{S} \in \mathbb{R}^{n \times 1}$ depends on the eigenvector \mathbf{y}_S and on the initial prestress level S

$$\mathbf{S} = \mathbf{y}_S S \quad (2.2)$$

The range of initial prestress level S is a property of the structure and depends on its characteristics and external load. The minimum prestress level S_{min} is related to the appropriate distribution of normal forces in the elements of the structure. The external load can cause a different distribution of normal forces, and it can be corrected by the introduction of a proper initial prestress level. In turn, the maximum prestress level S_{max} is related to the load-bearing capacity of the most stressed elements.

The aim of the paper is to assess the impact of prestress level on the dynamic behaviour of tensegrity domes under time-independent external loads $\mathbf{P} \in \mathbb{R}^{m \times 1}$. The most interesting for all are tensegrity domes characterized by the occurrence of infinitesimal mechanisms. In the absence of the initial prestress forces such systems are unstable, i.e., geometrically variable. The stabilization occurs only after the introduction of initial prestress. It should be noted, the mechanism is an eigenvector $\mathbf{x}_S \in \mathbb{R}^{m \times 1}$ related to the zero eigenvalue of the matrix $\mathbf{B}^T \mathbf{B} \in \mathbb{R}^{m \times m}$. The modification of the initial prestress level S allows for control, among others, dynamic parameters of the structure. In the paper, natural vibrations and free vibrations (taking into account the impact of the load, which is treated as the initial disturbance of the equilibrium state, i.e., as imposition of the initial conditions) are considered. The frequencies of vibrations are determined using the modal analysis

$$[\mathbf{K}_L + \mathbf{K}_G - (2\pi f)^2 \mathbf{M}] \tilde{\mathbf{q}} = \mathbf{0} \quad (2.3)$$

where $\mathbf{K}_L = \mathbf{B}^T \mathbf{E} \mathbf{B} \in \mathbb{R}^{m \times m}$ is a linear stiffness matrix, $\mathbf{M} \in \mathbb{R}^{m \times m}$ is a consequent mass matrix, f is the natural ($f_i(0)$) or free ($f_i(P)$) frequency of vibrations, $\tilde{\mathbf{q}}$ is an amplitude vector and $\mathbf{K}_G \in \mathbb{R}^{m \times m}$ is a geometry stiffness matrix.

In the case of natural vibrations, the geometry stiffness matrix depends only on the self-equilibrium system of longitudinal forces \mathbf{S} (2.2), consequently $\mathbf{K}_G = \mathbf{K}_G(\mathbf{S})$. For tensegrity domes characterized by infinitesimal mechanisms, the omission of the influence of prestress ($\mathbf{S} = \mathbf{0}$) in Eq. (2.3) leads to zero natural frequencies. The number of them is equal to the number of the infinitesimal mechanisms, and the forms of vibrations correspond to the forms of mechanisms. In the case of free vibrations, the geometry stiffness matrix depends additionally on the longitudinal forces $\mathbf{N} \in \mathbb{R}^{n \times 1}$ caused by the external load

$$\mathbf{K}_G = \mathbf{K}_G(\mathbf{S}) + \mathbf{K}_{GN}(\mathbf{N}) \quad (2.4)$$

Another specific property of tensegrity systems is the size of displacements, which can be large even with small deformations. Due to this, to calculate the axial forces, a geometrically non-linear model is used, assuming the hypothesis of large displacements. The non-linear theory of elasticity in terms of the Total Lagrangian (TL) was adopted as the basis for formulating tensegrity lattice equations

$$[\mathbf{K}_L + \mathbf{K}_G + \mathbf{K}_{NL}(\mathbf{q})] \mathbf{q} = \mathbf{P} \quad (2.5)$$

where $\mathbf{K}_{NL}(\mathbf{q}) \in \mathbb{R}^{m \times m}$ is a non-linear displacement stiffness matrix. The explicit forms of the matrices mentioned above can be found, for example, in (Obara, 2019).

3. Results and discussion

The paper presents dynamic parametric analyzes of two of the most well-known tensegrity domes, i.e., the Levy dome and Geiger dome. The domes consist of uniformly distributed systems of load-bearing girders. Comparing the geometry of both domes, significant differences can be noticed. In the case of the Levy dome, the load-bearing girders are spatial (Figs. 1a,b) whereas in the case of the Geiger dome – flat (Figs. 1c,d). The load-bearing girders consist of tensioned cables

(elements: 1-6) and compressed struts (elements: S_1, S_2, S_3), which are connected by additional circumferential cables (elements: C_1 - C_6). The node coordinates of the load-bearing girders are presented in Table 1 – diameter of 12 m and height of 3.25 m of all domes were adopted. The domes are supported in every external node of the lower section.

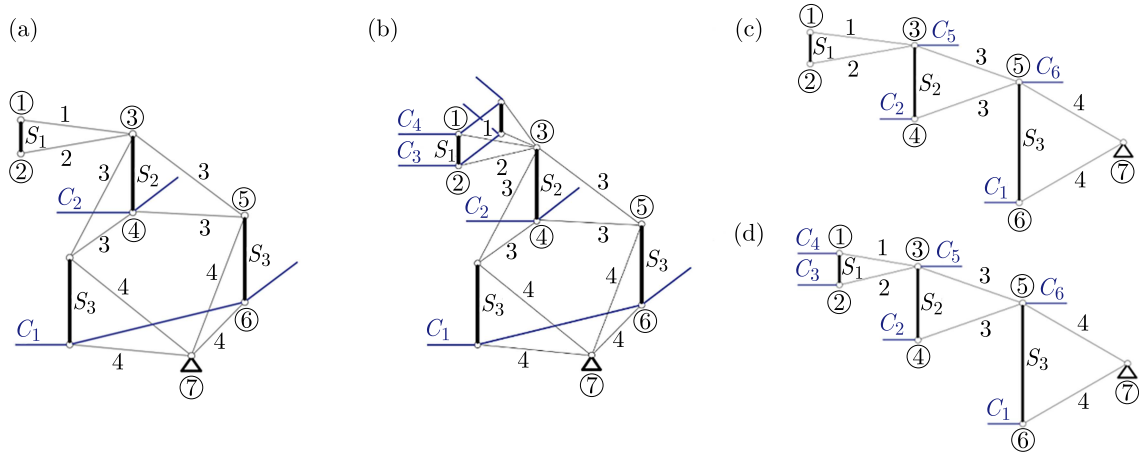


Fig. 1. Load-bearing girders of: (a) Levy type A, (b) Levy type B, (c) Geiger type A, (d) Geiger type B

Table 1. Node coordinates [m] of the load-bearing girders

No. nodes	Type of girder	1	2	3	4	5	6	7
x	A	0.0	0.0	2.0	2.0	4.0	4.0	6.0
	B	0.5	0.5					
z	A and B	2.1	1.5	1.85	0.45	1.15	-1.15	0.0

It should be noted, see the literature, there are two design solutions in the case of Geiger dome – regular (Yuan *et al.*, 2007; Kim and Sin, 2014; Qin *et al.*, 2023) and modified (Atig *et al.*, 2017). The comparison of both of them, in the natural frequency range, was the subject of our previous studies (Obara and Solovei, 2023). In this paper, due to being more similar to the Levy dome, a modified solution was chosen. The considerations contain two cases of configurations, i.e., type A – with a closed upper section (Figs. 1a and 1c) and type B – with an open upper section (Figs. 1b and 1d) and a different number of load-bearing girders i.e., 6 (Figs. 2a, 2c, 3a, 3c), 8, 10 and 12 (Figs. 2b, 2d, 3b, 3d). The names of analyzed domes are acronyms: G – Geiger dome, L – Levy dome, the number – the number of load-bearing girders and letter A or B – girders type e.g., “L 6A” is the Levy dome with 6 girders type A.

In order to compare the behaviour of both domes, the same maximum prestress level $S_{max} = 50$ kN was adopted (due to the maximum effort of the cables of the Geiger dome $W_{max} = 0.93$). In turn, the minimum prestress level S_{min} is an individual characteristic for every dome. Wherein, in the case of natural vibrations, the minimum prestress value is assumed as $S_{min} = 0$ kN.

3.1. Identification of self-stress states and infinitesimal mechanisms

The first step in the analysis of the Levy and Geiger domes is the identification of immanent features of tensegrity structures, such as infinitesimal mechanisms and self-stress states. The results of this analysis are shown in Table 2. The domes differ in the number of these features. The Levy dome type A are characterized by zero mechanisms and type B by 1 mechanism,

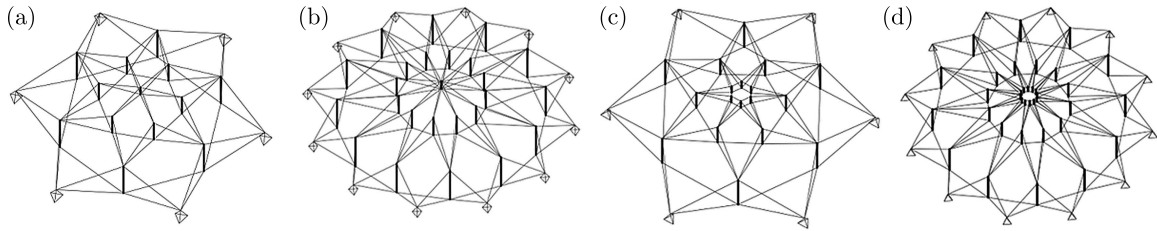


Fig. 2. Levy domes: (a) L 6A, (b) L 12A, (c) L 6B, (d) L 12B

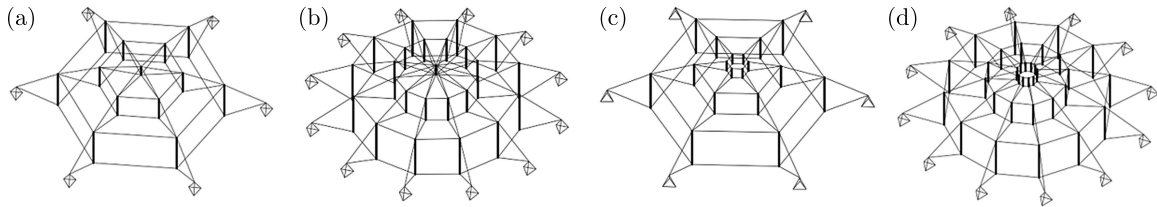


Fig. 3. Geiger domes: (a) G 6A, (b) G 12A, (c) G 6B, (d) G 12B

Table 2. Immanent features of tensegrity domes

Type and No. girders	No. nodes	Levy dome			Geiger dome			
		No. elements	No. mechanisms	No. self-stress states	No. elements	No. Mechanisms	No. self-stress states	
A	6	32	85	0	7	73	8	3
	8	42	113	0	11	97	8	3
	10	52	141	0	15	121	8	3
	12	62	169	0	19	145	8	3
B	6	42	114	1	7	90	21	3
	8	56	152	1	9	120	27	3
	10	70	190	1	11	150	33	3
	12	84	228	1	13	180	39	3

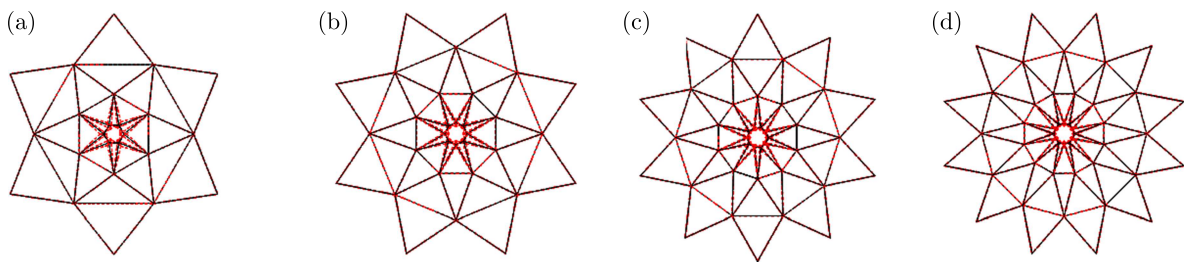


Fig. 4. Infinitesimal mechanism of domes: (a) L 6B, (b) L 8B, (c) L 10B, (d) L 12B

regardless of the number of girders. It should be noted that the mechanism is related only to the upper section (Fig. 4). In turn, in the case of Geiger dome, the number of mechanisms increases with the number of girders. The type of mechanisms differs in the case of the Levy dome – it is related to the entire structure (Fig. 5). In turn, in the case of self-stress states, their number does not depend on the number of girders in the case of Geiger dome (always equals three). In the case of the Levy dome, the number of self-stress states increases with the number of girders. Unfortunately, none of the identified self-stress states identify the type of elements properly. A superposition is needed. The superposed values of self-stress states y_S for the Levy and Geiger domes are presented in Tables 3 and 4, respectively.

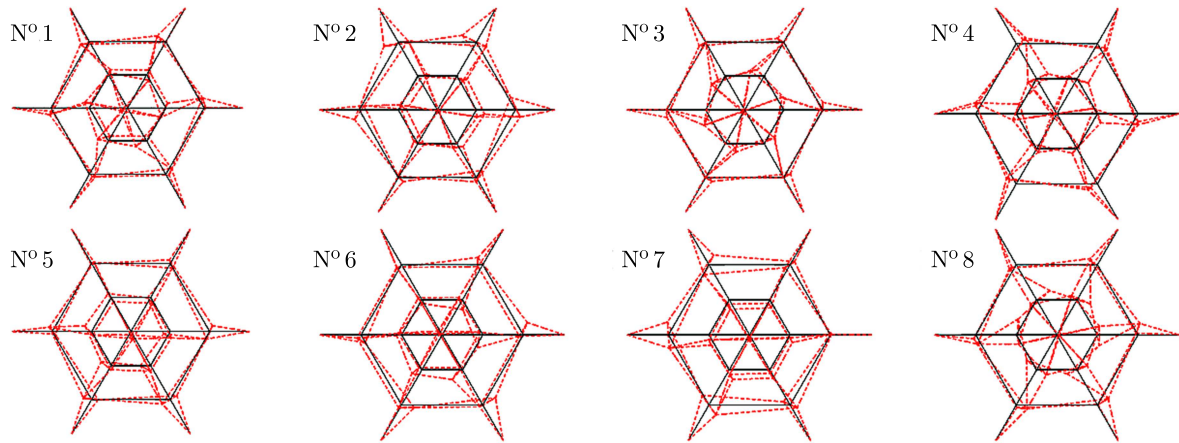


Fig. 5. Infinitesimal mechanisms of dome G 6A

Table 3. Values of self-stress state \mathbf{y}_S of Levy domes

Type A						Type B					
el.	\mathbf{y}_S	el.	\mathbf{y}_S	el.	\mathbf{y}_S	el.	\mathbf{y}_S	el.	\mathbf{y}_S	el.	\mathbf{y}_S
S_1	$-0.147^{(6)}$	1	$0.197^{(6)}$	C_1	$1.040^{(6)}$	S_1	$-0.031^{(6)}$	1	$0.100^{(6)}$	C_1	$1.040^{(6)}$
	$-0.308^{(8)}$		$0.311^{(8)}$		$1.753^{(8)}$		$-0.050^{(8)}$		$0.157^{(8)}$		$1.753^{(8)}$
	$-0.465^{(10)}$		$0.375^{(10)}$		$2.401^{(10)}$		$-0.061^{(10)}$		$0.189^{(10)}$		$2.401^{(10)}$
	$-0.616^{(12)}$		$0.414^{(12)}$		$3.016^{(12)}$		$-0.068^{(12)}$		$0.209^{(12)}$		$3.016^{(12)}$
S_2	$-0.161^{(6)}$	2	$0.142^{(6)}$	C_2	$0.336^{(6)}$	S_2	$-0.161^{(6)}$	2	$0.073^{(6)}$	C_2	$0.336^{(6)}$
	$-0.218^{(8)}$		$0.224^{(8)}$		$0.691^{(8)}$		$-0.218^{(8)}$		$0.114^{(8)}$		$0.691^{(8)}$
	$-0.248^{(10)}$		$0.270^{(10)}$		$1.032^{(10)}$		$-0.248^{(10)}$		$0.137^{(10)}$		$1.032^{(10)}$
	$-0.264^{(12)}$		$0.298^{(12)}$		$1.359^{(12)}$		$-0.264^{(12)}$		$0.151^{(12)}$		$1.359^{(12)}$
S_3	-1.000	3	$0.295^{(6)}$	C_3		S_3	-1.000	3	$0.295^{(6)}$	C_3	$0.109^{(6)}$
			$0.372^{(8)}$		$0.252^{(8)}$						
			$0.406^{(10)}$		$0.396^{(10)}$						
			$0.424^{(12)}$		$0.534^{(12)}$						
		4	$1.491^{(6)}$	C_4				4	$1.491^{(6)}$	C_4	$0.154^{(6)}$
			$1.303^{(8)}$		$0.353^{(8)}$						
			$1.204^{(10)}$		$0.554^{(10)}$						
			$1.147^{(12)}$		$0.748^{(12)}$						

⁽⁶⁾ dome with 6 girders; ⁽⁸⁾ dome with 8 girders;

⁽¹⁰⁾ dome with 10 girders; ⁽¹²⁾ dome with 12 girders

3.2. Influence of the number of girders on natural frequencies

After the identification of self-stress states and infinitesimal mechanisms, the influence of initial prestress level S on the natural frequencies is considered. Particularly, the impact of the number of girders on the frequencies is analyzed. It is assumed that the cables are made of steel S460N. Type A cables with Young's modulus 210 GPa (EN 1993-1-11: 2006) are used. The cable diameter and load-bearing capacity are 20 mm and 110.2 kN, respectively. The struts are made of hot-finished circular hollow sections (steel S355J2) with Young's modulus 210 GPa. The diameter and thickness of struts are 76.1 mm and 2.9 mm, respectively. The struts were divided into three groups according to length and load-bearing capacity. Group 1 lengths are 0.6 m and $N_{Rd} = 224.3$ kN, group 2 are 1.4 m and 170.5 kN, and group 3 are 2.3 m and 107.1 kN. The density of steel is equal to $\rho = 7860$ kg/m³. The calculations were made using quasi-linear and non-linear models implemented in the Mathematica environment.

Table 4. Values of self-stress state \mathbf{y}_S of Geiger domes

Type A						Type B					
el.	\mathbf{y}_S	el.	\mathbf{y}_S	el.	\mathbf{y}_S	el.	\mathbf{y}_S	el.	\mathbf{y}_S	el.	\mathbf{y}_S
S_1	$-0.228^{(6)}$	1	0.306	C_1	$1.739^{(6)}$	S_1	-0.051	1	0.308	C_1	$1.739^{(6)}$
	$-0.304^{(8)}$				$2.272^{(8)}$						$2.272^{(8)}$
	$-0.380^{(10)}$				$2.814^{(10)}$						$2.814^{(10)}$
	$-0.455^{(12)}$				$3.360^{(12)}$						$3.360^{(12)}$
S_2	-0.265	2	0.220	C_2	$0.756^{(6)}$	S_2	-0.265	2	0.223	C_2	$0.756^{(6)}$
					$0.988^{(8)}$						$0.988^{(8)}$
					$1.223^{(10)}$						$1.223^{(10)}$
					$1.461^{(12)}$						$1.461^{(12)}$
S_3	-1.000	3	0.801	C_3		S_3	-1.000	3	0.801	C_3	$0.217^{(6)}$
											$0.283^{(8)}$
											$0.351^{(10)}$
											$0.419^{(12)}$
		4	2.006	C_4			4	2.006	C_4	$0.303^{(6)}$	
					$0.396^{(8)}$						
					$0.491^{(10)}$						
					$0.586^{(12)}$						
				C_5	$0.236^{(6)}$				C_5	$0.236^{(6)}$	
					$0.308^{(8)}$	$0.308^{(8)}$					
					$0.381^{(10)}$	$0.381^{(10)}$					
					$0.455^{(12)}$	$0.455^{(12)}$					
				C_6	$0.227^{(6)}$				C_6	$0.227^{(6)}$	
					$0.297^{(8)}$	$0.297^{(8)}$					
					$0.368^{(10)}$	$0.368^{(10)}$					
					$0.439^{(12)}$	$0.439^{(12)}$					

⁽⁶⁾ dome with 6 girders; ⁽⁸⁾ dome with 8 girders;

⁽¹⁰⁾ dome with 10 girders; ⁽¹²⁾ dome with 12 girders

The first part of the assessment concerns the influence of initial prestress level S on natural frequencies $f_i(0)$. The dynamic behaviour of the dome is highly dependent on the type of load-bearing girder and on the number of identified infinitesimal mechanisms. In Fig. 6, the first and last frequencies corresponding to the infinitesimal mechanisms are presented. The zero level of initial prestress leads to zero natural frequencies, however, they increase with an initial prestress level. The range of changes mainly depends on the kind of dome, which means, on the number of mechanisms. In the case of the dome with one mechanism, i.e., Levy domes type B (Fig. 6a), the first frequency for S_{max} is 17.62 Hz (L 6B), 30.49 Hz (L 8B), 42.28 Hz (L 10B) and 54.2 Hz (L 12B), which means that with the number of girds the frequency increases (comparing with L 6B) by 73%, 140% and 208%, respectively. In turn, for domes with eight mechanisms, i.e., Geiger domes type A (Fig. 6b), the influence of the number of girders on frequencies is significantly smaller. For example, the value of eighth frequency f_8 for S_{max} varies within the range of 12.3 Hz (G 6A) to 13.7 Hz (G 12A), this means an increase of up 11%. In the case of the Geiger domes type B (Fig. 6b) with a different number of infinitesimal mechanisms, the influence of the number of girders depends on the frequency. The first natural frequency for all domes is almost the same – $f_1(S_{max}) = 5.1$ Hz to 5.6 Hz but the last frequency, which corresponds to the mechanism, for S_{max} is 29.79 Hz (G 6B), 35.94 Hz (G 8B), 48.31 Hz (G 10B) and 57.83 Hz (G 12B), which means that with growing number of girds the frequency increases (comparing with G 6B) by 21%, 62% and 94%, respectively. Additionally, as can be seen, for Geiger domes type B, the higher frequencies are more sensitive to a change in prestressing.

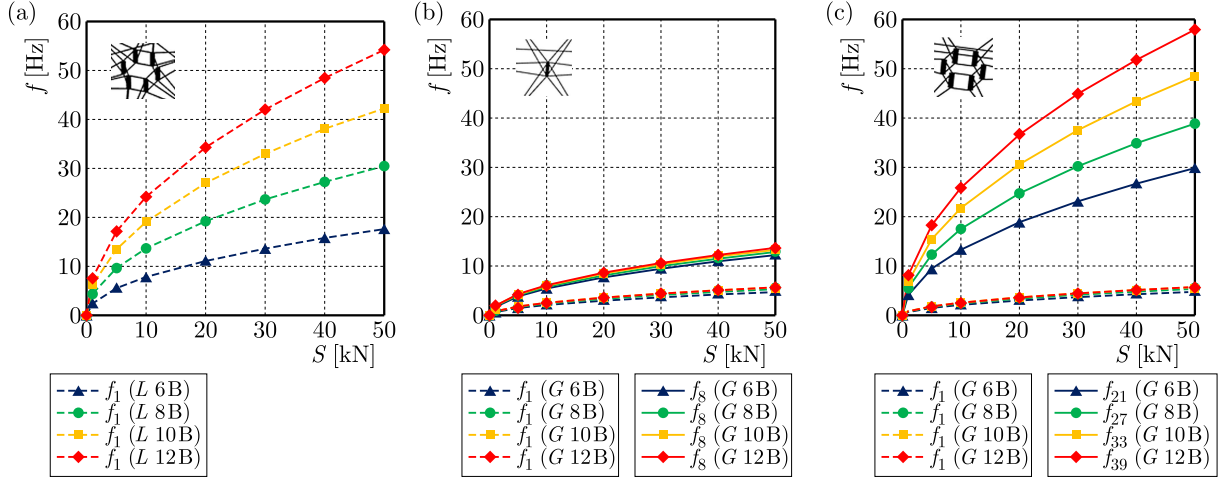


Fig. 6. Natural frequencies corresponding to the infinitesimal mechanisms: (a) Levy domes type B, (b) Geiger domes type A, (c) Geiger domes type B

It is well known that the number of natural frequencies, depending on prestressing, is equal to the number of infinitesimal mechanisms f_{nm} , but in the case of Levy dome type B and Geiger domes of type A, it is different. These structures are characterized by additional natural frequencies f_{add} . The number of them, and the sensitivity to the initial prestress changes, depends on the number of load-bearing girders $No.g$

$$f_{add} = \begin{cases} No.g - 4 & \text{for Levy domes} \\ No.g - 3 & \text{for Geiger domes} \end{cases} \quad (3.1)$$

For comparison, the sensitivity to the prestress changes, in Figs. 7 and 8, the last frequency corresponding to the infinitesimal mechanism, the additional depending on prestress and the first independent of prestress are shown. In the absence of prestress, the additional frequencies, unlike the frequency corresponding to the mechanism, are not zero and the character of the dependence on prestress relies on the types of domes. In the case of Levy domes (Fig. 7), the additional frequencies are more sensitive to a change in prestressing than in the case of Geiger domes (Fig. 8). Additionally, the nature of changes is different. First, for Geiger domes, the additional frequencies are directly proportional to the initial prestress level, whereas in the case of Levy domes, they are not. Secondly, the influence of the number of girders on the frequency is more significant in Levy domes. Thirdly, for Geiger domes, regardless of the number of girders, the value of the frequency independent of prestress is much higher than the frequencies dependent on prestress.

The behaviour of the Levy domes type A is completely different, compared to the Levy dome type B and Geiger domes of type A and B. In these domes, the mechanism was not identified. In Fig. 9, the influence of the initial prestress S on the first, second, and third frequency is shown. The dependencies are linear and almost constant, especially for domes with a small number of girders. In the case of the first frequency, with a growth of the prestress from S_{min} to S_{max} , the frequency increased only by 6.4% (L 6A), 6% (L 8A), 7% (L 10A), and 8.3% (L 12A), whereas in the case of the third frequency – 0.4% (L 6A), 3.5% (L 8A), 5.1% (L 10A), and 6.4% (L 12A). Comparing all results, we can say that due to the lack of mechanisms in the case of Levy dome type A, the natural frequencies are practically not affected by the initial prestress, independent of the number of load-bearing girders.

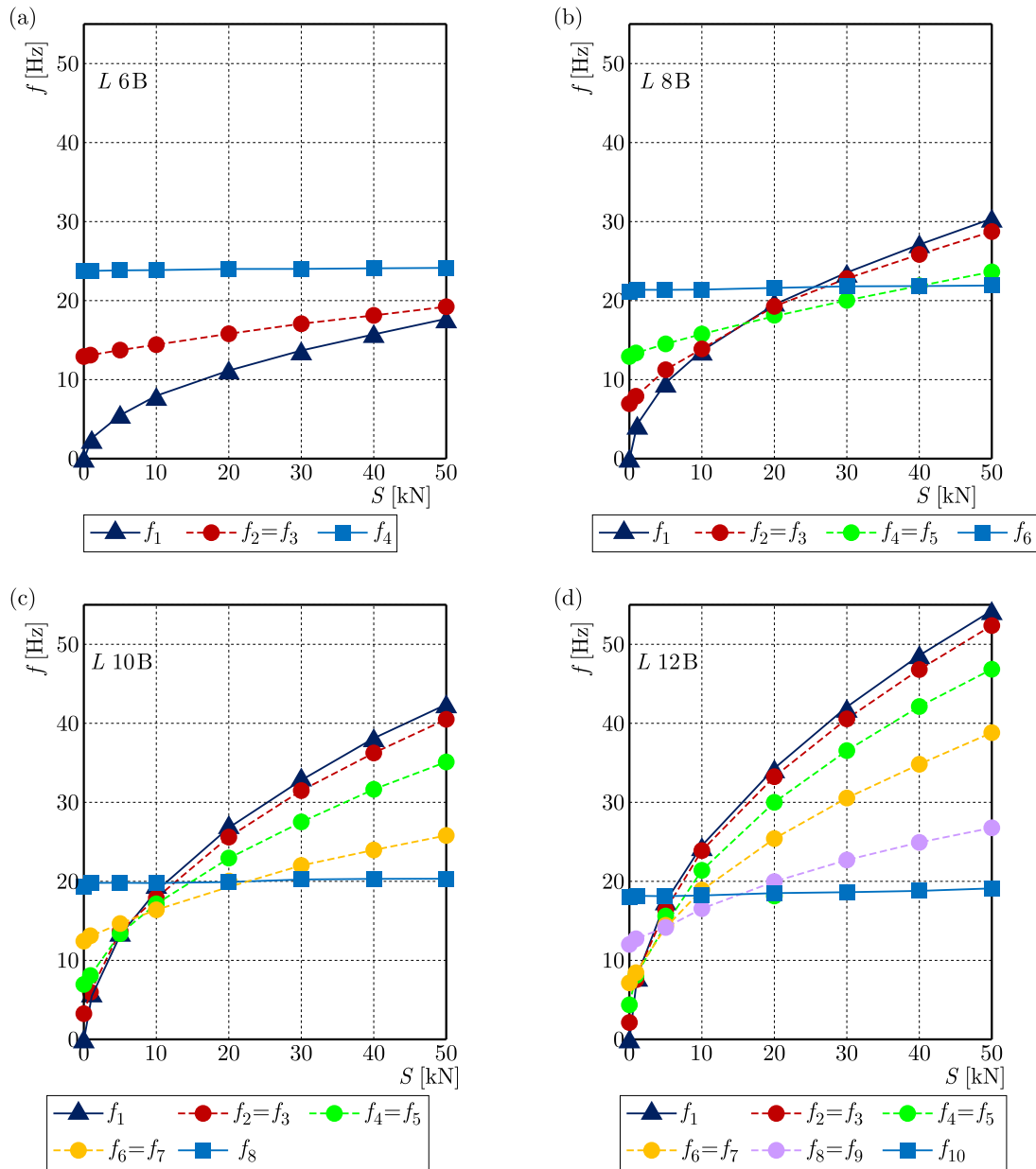


Fig. 7. Influence of the initial prestress S on the natural frequency for Levy domes type B: (a) L 6B, (b) L 8B, (c) L 10B, (d) L 12B

3.3. Influence of the initial prestress level on free frequencies

Next, the influence of initial prestress level S on the free $f_i(P)$ frequencies of the domes is calculated. The time-independent concentrated force applied vertically (gravity load) to one top node is considered. Two variants of loads i.e., $P = 1$ kN and $P = 5$ kN are taken into account. To compare the response to external disturbance, the load is applied in three different positions. The first position is a node of the upper section of the dome, the second position corresponds with a node on the hoop of the second section, and the third one – is with the third section, respectively. It means, according to Fig. 1, that the load is applied to the 1st, 3rd, and 5th node. It should be noted that taking into account the external load, the initial conditions change, and the influence of initial prestress decreases. The load causes additional stress in the system and it is necessary to determine the minimum prestress level S_{min} . S_{min} must ensure the appropriate identification of the element type and provide the positive definite matrix. This is calculated

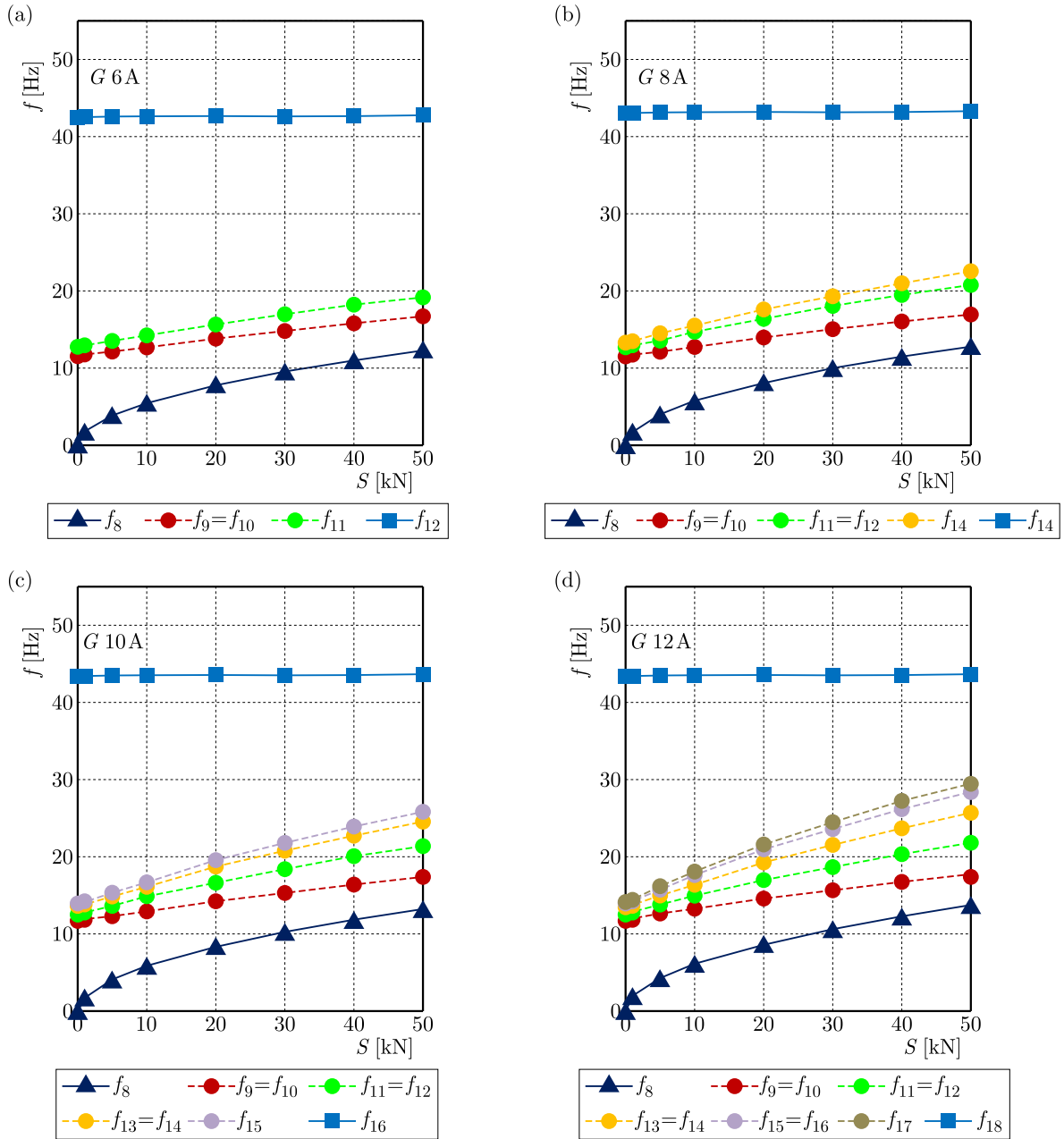


Fig. 8. Influence of the initial prestress S on the natural frequency for Geiger domes type A: (a) G 6A, (b) G 8A, (c) G 10A, (d) G 12A

individually for each dome for each variant of the load. As an example, the results of the analysis of domes with 6 load-bearing girders are shown (Tables 5-8).

In the case of Levy domes type A, the first natural $f_1(0)$ and free $f_1(P)$ frequencies are shown in Table 5. Due to the lack of mechanisms, the free frequencies, like natural ones, are practically not affected by the initial prestress, and are independent of the number of load-bearing girders. The natural frequencies are the same as natural ones. The only thing that changes is the lowest level of initial prestress. It depends not only value of the load but also on the number of loaded nodes. The second position (3rd node) corresponding with a node on the hoop of the second section is the worst, and S_{min} level is only 42 kN. The first position (1st node) corresponds with a node of the upper section of the dome, and S_{min} is equal to 18 kN. The third position (5th node) corresponds with a node of third section, and S_{min} is equal to 5 kN.

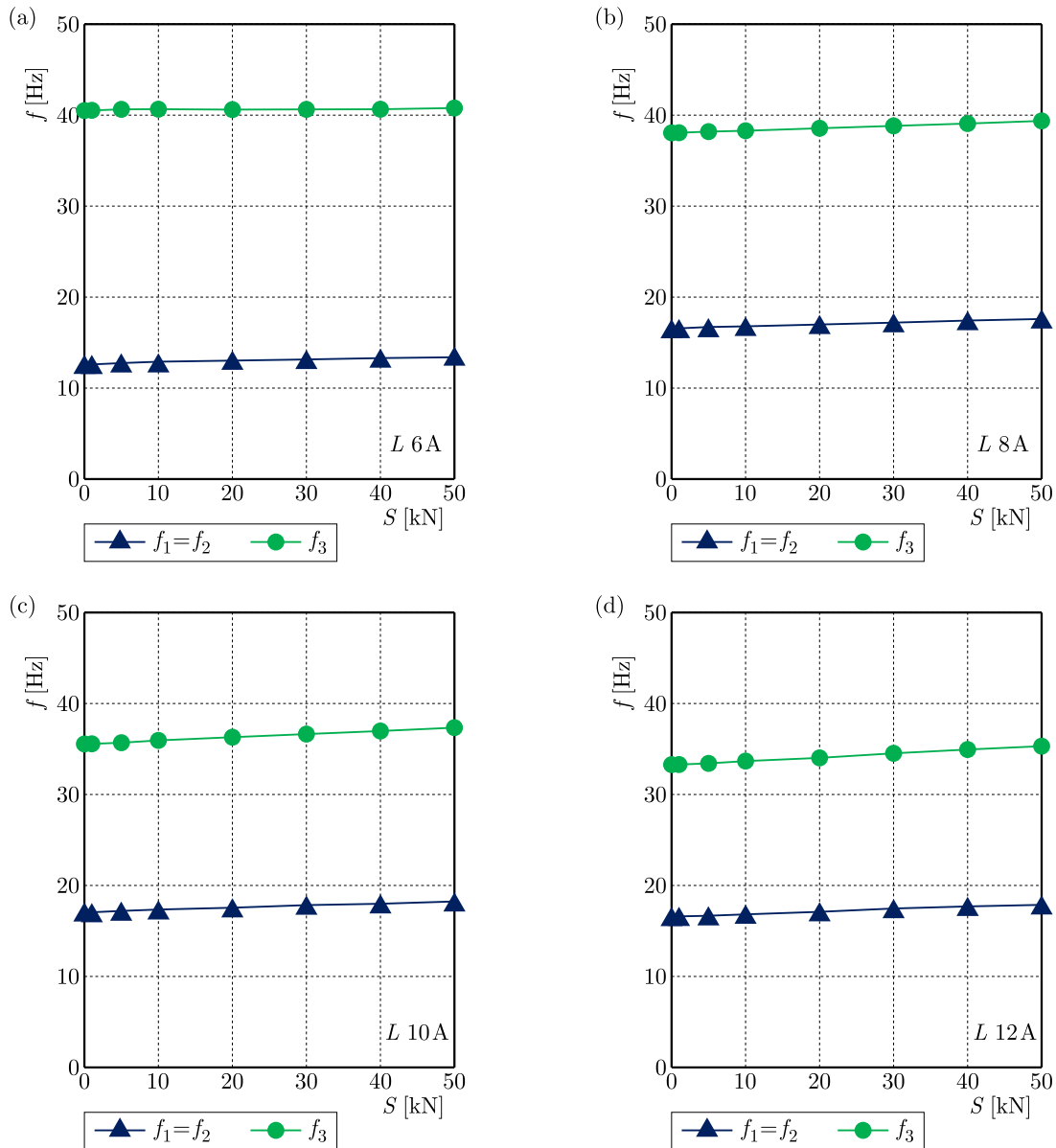


Fig. 9. Influence of the initial prestress S on the natural frequency for Levy domes type A: (a) L 6A, (b) L 8A, (c) L 10A, (d) L 12A

In the case of Levy domes type B, the first natural $f_1(0)$ and free $f_1(P)$ frequencies corresponding to the one identified mechanism are shown in Table 6. The external force placed in the first position (1st node) corresponds with a node of the upper section of the dome causing too much disturbance of the equilibrium state, and it is impossible to obtain the minimal prestress. The second position (3rd node) corresponds with a node on the hoop of the second section, and S_{min} is equal to 50 kN. The third position (5th node) corresponds with a node of the third section, and S_{min} is equal to 12 kN. The free frequencies are changing almost linearly.

In turn, in the case of Geiger domes, the first and last natural $f_i(0)$ and free $f_i(P)$ frequencies corresponding to the mechanisms are presented in Table 7 (for domes type A) and in Table 8 (for domes type B). For the Geiger domes type A, the third position (5th node) corresponding with a node of the third section is the worst, and S_{min} is equal to 36 kN, for both free and natural frequencies. The second position (3rd node) corresponds with a node on the hoop of the second section, and S_{min} is equal to 34 kN. The first position (1st node) corresponds with a node of the

Table 5. First natural $f_1(0)$ and free $f_1(P)$ frequency [Hz] for dome L 6A

S [kN]	$f_1(0)$	$f_1(P)$					
		1st node		3rd node		5th node	
		1 kN	5 kN	1 kN	5 kN	1 kN	5 kN
0	12.84						
1	12.86					12.86	
4	12.91	12.91				12.91	
5	12.92	12.92				12.92	12.92
9	12.99	12.99		12.99		12.99	12.99
10	13.01	13.01		13.00		13.01	13.00
18	13.14	13.14	13.14	13.14		13.14	13.13
20	13.17	13.18	13.18	13.17		13.18	13.17
30	13.34	13.34	13.34	13.34		13.34	13.33
40	13.50	13.50	13.51	13.50		13.50	13.50
42	13.53	13.54	13.53	13.54	13.52	13.53	13.53
50	13.66	13.67	13.67	13.66	13.65	13.66	13.66

Table 6. First natural $f_1(0)$ and free $f_1(P)$ frequency [Hz] for dome L 6B

S [kN]	$f_1(0)$	$f_1(P)$					
		1st node		3rd node		5th node	
		1 kN	5 kN	1 kN	5 kN	1 kN	5 kN
0	0.00						
1	2.49						
3	4.32					4.23	
5	5.57					5.49	
10	7.88			7.51		7.84	
12	8.63			8.29		8.56	8.26
20	11.15			10.88		11.11	10.84
22	11.69	11.54		11.38		11.64	11.35
30	13.65	13.53		13.42		13.62	13.38
40	15.76	15.65		18.04		15.74	15.49
50	17.62	17.53		19.12	15.53	17.59	17.34

upper section of the dome, and S_{min} is equal to 11 kN. However, for the Geiger dome type B, the first position (1st node) corresponding with a node of the upper section is the worst, and S_{min} is equal to 41 kN. The second position (3rd node) corresponds with a node on the hoop of the second section, and S_{min} is equal to 26 kN. The third position (5th node) corresponds with a node of the third section, and S_{min} is equal to 2 kN.

4. Conclusions

In this paper, the dynamic behaviour of tensegrity domes is explored. It is well known that the number of prestress-dependent frequencies is equal to the number of infinitesimal mechanisms. In the absence of prestress, these frequencies are zero, and the corresponding forms of vibrations implement the mechanisms. After introducing the initial prestress, the frequencies increase. If several mechanisms are identified, the higher frequencies are more sensitive to the initial prestress changes. The sensitivity of these natural frequencies to the initial prestress is so great that the

Table 7. Natural $f_i(0)$ and free $f_i(P)$ frequency [Hz] for dome G 6A

S [kN]	$f_1(0)$	$f_1(P)$						$f_8(0)$	$f_8(P)$					
		1st node		3rd node		5th node			1st node		3rd node		5th node	
		1 kN	5 kN	1 kN	5 kN	1 kN	5 kN		1 kN	5 kN	1 kN	5 kN	1 kN	5 kN
0	0.00							0.00						
1	0.73							1.75						
3	1.26	1.19						3.03	3.02					
5	1.62	1.56						3.91	3.90					
8	2.05	1.99		2.08				4.95	4.94		5.27			
10	2.30	2.26		2.31				5.52	5.52		5.73			
11	2.41	2.35	2.22	2.39				5.79	5.79	5.79	5.95			
12	2.51	2.46	2.34	2.49		2.51		6.05	6.05	6.05	6.17		6.06	
20	3.25	3.22	3.12	3.23		3.23		7.81	7.81	7.80	7.85		7.80	
30	3.98	3.96	3.88	3.96		3.96		9.57	9.56	9.55	9.58		9.56	
34	4.23	4.22	4.19	4.20	4.20	4.23		10.19	10.18	10.17	10.22	10.44	10.25	
36	4.36	4.35	4.33	4.32	4.32	4.36	4.31	10.48	10.48	10.45	10.52	10.71	10.56	10.47
40	4.59	4.58	4.51	4.58	4.55	4.58	4.54	11.05	11.05	11.04	11.05	11.22	11.04	11.03
50	5.13	5.12	5.06	5.12	5.08	5.12	5.09	12.35	12.35	12.34	12.35	12.45	12.34	12.32

Table 8. Natural $f_i(0)$ and free $f_i(P)$ frequency [Hz] for dome G 6B

S [kN]	$f_1(0)$	$f_1(P)$						$f_8(0)$	$f_8(P)$					
		1st node		3rd node		5th node			1st node		3rd node		5th node	
		1 kN	5 kN	1 kN	5 kN	1 kN	5 kN		1 kN	5 kN	1 kN	5 kN	1 kN	5 kN
0	0.00							0.00						
1	0.72							4.21						
2	1.02					1.41	2.16	5.96					8.64	13.21
5	1.61					1.76	2.33	9.42					10.56	14.20
10	2.28			2.32		2.29	2.61	13.32			13.56		13.52	15.87
14	2.70	2.69		2.72		2.66	2.92	15.77	18.91		15.71		15.66	17.45
20	3.23	3.22		3.22		3.13	3.28	18.84	20.72		18.77		18.85	19.61
26	3.68	3.67		3.55	3.72	3.69	3.68	21.48	22.67		21.33	21.65	21.47	21.65
30	3.96	3.94		3.94	3.97	3.94	3.94	23.08	23.92		22.97	23.08	23.06	23.33
40	4.57	4.55		4.55	4.54	4.56	4.53	26.65	27.06		26.54	26.42	26.63	26.72
41	4.62	4.61	4.57	4.61	4.58	4.69	4.59	26.98	27.31	32.27	26.97	26.79	27.16	26.91
50	5.11	5.09	5.06	5.09	5.07	5.10	5.06	29.79	30.01	33.81	29.69	29.47	29.77	29.79

change in the level of prestress can be successfully used to control the dynamic properties of the structure. Theoretically, other frequencies should be practically insensitive to self-stress changes. However, in the case of some analyzed domes, i.e., Levy domes type B and Geiger domes type A, it is different. There are additional frequencies that depend on the initial prestress. In the absence of prestress, the additional frequencies, unlike to frequency corresponding to the mechanism, are not zero. The number of them, and the sensitivity to initial prestress changes, depends on the kind of dome and number of girders.

Comparing all the results, we can say that due to the lack of the mechanisms, i.e., Levy dome type A, the natural and free frequencies are practically not affected by the initial prestress, independent of the number of load-bearing girders.

The considerations contained in this paper indicate the unusual behaviour of tensegrity domes. The obtained results are important for dynamic stability analysis of behaviour of tensegrity

rity structures under periodic loads, which will be the subject of feature investigation. The dynamic stability analysis cannot be carried out without the analysis presented in this paper.

References

1. ARSENAULT M., GOSSELIN C.M., 2005, Kinematic, static, and dynamic analysis of a planar one-degree-of-freedom tensegrity mechanism, *Journal of Mechanical Design*, **127**, 6, 1152-1160
2. ATIG M., EL OUNI M.H., KAHLA N.B., 2017, Dynamic stability analysis of tensegrity systems, *European Journal of Environmental and Civil Engineering*, **23**, 6, 675-692
3. BEL HADJ ALI N., RHODE-BARBARIGOS L., SMITH I.F.C., 2010, Analysis of clustered tensegrity structures using a modified dynamic relaxation algorithm, *International Journal of Solids and Structures*, **48**, 5, 637-647
4. EN 1993-1-11, 2006, Eurocode 3: Design of steel structures – Part 1-11: Design of structures with tension components
5. GEIGER D.H., 1988, *Roof Structure*, U.S. Patent 4 736 553
6. GEIGER D.H., STEFANIUK A., CHEN D., 1986, The design and construction of two cable domes for the Korean Olympics, *Proceeding of the IASS Symposium on Shells, Membranes and Space Frames*, Osaka, Japan, 265-272
7. GILEWSKI W., KŁOSOWSKA J., OBARA P., 2016, Form finding of tensegrity structures via Singular Value Decomposition, *Advances in Mechanics: Theoretical, Computational and Interdisciplinary Issues*, 191-195
8. KAWAGUCHI M., TATEMACHI I., CHEN P.S., 1999, Optimum shapes of a cable dome structure, *Engineering Structures*, **21**, 8, 719-725
9. KIM S.-D., SIN I.-A., 2014, A comparative analysis of dynamic instability characteristic of Geiger-typed cable dome structures by load condition, *Journal of the Korean Association for Spatial Structures*, **14**, 1, 85-91
10. LEE J., TRAN H.C., LEE K., 2009, Advanced form-finding for cable dome structures, *Proceeding of IASS Symposium*, 2116-2127
11. LEVY M.P., 1989, Hypar-tensegrity dome, *Proceeding of International Symposium on Sports Architecture*, Beijing, China, 157-162
12. LEVY M.P., 1994, The Georgia dome and beyond: achieving lightweight-longspan structures, *Proceedings of the IASS-ASCE International Symposium*, Atlanta, USA, 560-562
13. LEVY M., JING T.-F., BRZozowski A., FREEMAN G., 2013, Estadio ciudad de La Plata (La Plata Stadium), *Structural Engineering International*, **23**, 303-310
14. LI Q., SKELTON R.E., YAN J., 2011, Energy optimization of deployable tensegrity structure, *Proceeding of the 30th Chinese Control Conference*, Yantai, China, 12383827
15. MA Q., OHSAKI M., CHEN Z., YAN X., 2018, Step-by-step unbalanced force iteration method for cable-strut structure with irregular shape, *Engineering Structures*, **177**, 331-344
16. OBARA P., 2019, *Dynamic and Dynamic Stability of Tensegrity Structures* (in Polish), Wydawnictwo Politechniki Świętokrzyskiej, Kielce, Poland
17. OBARA P., SOLOVEI M., 2023, Assessment of the impact of the number of girders on the dynamic behaviour of Geiger dome, *Archives of Civil Engineering*, **69**, 3, 597-611
18. OBARA P., SOLOVEI M., TOMASIK J., 2023a, Genetic algorithm as a tool for the determination of the self-stress states of tensegrity domes, *Applied Sciences*, **13**, 9, 5267
19. OBARA P., SOLOVEI M., TOMASIK J., 2023b, Qualitative and quantitative analysis of tensegrity steel domes, *Bulletin of Polish Academy of Sciences*, **71**, 1, 1-8

20. ORIBASI A., PARONESSO A., DAUNER H.-G., 2002, The new world cycling center in aigle, *Stahlbau*, **71**, 584-591
21. QIN W., GAO H., XI Z., FENG P., LI Y., 2023, Shaking table experimental investigations on dynamic characteristics of CFRP cable dome, *Engineering Structures*, **281**, 115748
22. REBIELAK J., 2000, Structural system of cable dome shaped by means of simple form of spatial hoops, *Proceeding of Lightweight Structures in Civil Engineering*, 114-115
23. SHEN X., ZHANG Q., LEE D.S.H., CAI J., FENG J., 2021, Static behavior of a retractable suspen-dome structure, *Symmetry*, **13**, 7, 1105
24. SUN G., XIAO S., XUE S., 2021, Test and numerical investigation mechanical behavior of cable dome, *International Journal of Steel Structures*, **21**, 4, 1502-1514, 2021
25. TRAN H.C., LEE J., 2013, Form-finding of tensegrity structures using double singular value decomposition, *Engineering with Computers*, **29**, 71-86
26. YUAN X., CHEN L., DONG S., 2007, Prestress design of cable domes with new forms, *International Journal of Solids and Structures*, **44**, 2773-2782
27. ZHANG P., FENG J., 2017, Initial prestress design and optimization of tensegrity systems based on symmetry and stiffness, *International Journal of Solids and Structures*, **106-107**, 68-90
28. ZHANG J.Y., OHSAKI M., 2006, Adaptive force density method for form-finding problem of tensegrity structures, *International Journal of Solids and Structures*, **43**, 18-19, 5658-5673
29. ZIENKIEWICZ O. C., TAYLOR R.L., 2000, *The Finite Element Method. Vol. 1. The Basis*, Elsevier Butterworth-Heinemann, London, Great Britain

Manuscript received October 30, 2023; accepted for print December 9, 2023